UDC 629.735.3 DOI: 10.30748/nitps.2017.28.04

R.M. Farhadi, V.I. Kortunov

Kharkiv National Aerospace University named after N. Zhukovsky (KhAI), Kharkov, Ukraine

ROBUST CONTROL DESIGN AND TESTING FOR AN UNMANNED AIR VEHICLE

In this paper, three robust control methods for the uncertain dynamic model of Skywalker X8 flying-wing unmanned air vehicle are designed: mu-synthesis, robust proportional integral derivative control and adaptive robust proportional integral derivative control using optimization. The implementation feasibility of designed robust control systems based on the capabilities of the autopilot hardware is investigated. A robust proportional integral derivative and robust adaptive proportional integral derivative control are designed based on the considerations of the robustness of the system's behavior as well as hardware considerations. With a robust control system based on mu-synthesis, it is possible to achieve better reference signal tracking and disturbance rejection. But the hardware processor speed of the existing autopilot makes it impossible to implement this controller. Two parallel microcontrollers or a dual-core microcontroller must be used to implement a control system based on the mu-synthesis. Designed robust adaptive proportional integral derivative controller for roll channel was implemented in the existing autopilot and tested in flight test. Flight test results with adaptive robust proportional integral derivative controller show better disturbance rejection in the roll channel than the traditional one.

Keywords: *robust control design, mu-synthesis, flying-wing unmanned air vehicle, robust and robust adaptive proportional integral derivative control, implementation of robust control system.*

Introduction

Robustness is one of the most fundamental issues in the design of control systems. Because, firstly, control systems are in effect exposed to noise measurement and external disturbances, and secondly, control systems are designed based on mathematical models that are different from the actual system. A control engineer should design a controller that can: 1. Stabilize the system. 2. Provide the expected level of performance in the presence of external disturbances, measurement noise, unmodified dynamics and system parameters change. These multiple targets are achieved through the feedback structure in the control system.

A robust control design refers to the controller design techniques that use information about uncertainty in modeling to ensure that robust performance features are provided. In single-input single-output systems, robustness is provided via the phase and gain margin, which guarantees somewhat optimal performance. With the development of multi-input multi-output systems, the methods provided did not guarantee the robustness of the system in order to guarantee optimal performance. These methods were based on a second-order cost function and Gaussian disturbance. Their performance is proven for systems that have a precise model and their noise and disturbances are white noise. But the application of these methods, generally called LQG, has not been very successful in the industry from the standpoint of robustness. This led to extensive researches to consider the need for robustness in the design process of the control system.

Initial work in the field of robust control design for multi-input-multi-output systems was done by Mr. Zames in the 1970s with the small gain theorem. His work set up an optimal H_∞ control method. The robust control theory based on the H_∞ optimization method and mu-synthesis and analysis is a systematic method for designing a robust control for multi-input multi-output systems. In this robust control method, the disadvantages of the two methods, the classic control (from 1950 to 1950), and the modern control (1950–1970), are compensated and the advantages of the two methods are used. H_∞ and mu-synthesis robust control, in contrast to the classic control design approach, can be used for multiple multi-input multi-output systems. However, at the same time, the frequency domain is still used in this method through the Bode and the Nyquist diagrams as in the design of the classic control. On the other hand, it eliminates the shortcomings of modern control by achieving robust stability and performance. It also uses computer abilities and modern design techniques. Table 1 presents the history of robust control development. In Table 1 is shown stages of the robust control development, [1–6].

Robust control based on H_∞ and mu-synthesis is designed for some flight altitudes and a range of variations in the airspeed of the flight vehicle in [7]. In [8] for the roll channel of the UAV is designed robust control based on H_∞ and mu-synthesis. In this paper, the uncertainty of the estimated aerodynamic coefficients is also added to the problem. Here, from the practical

point of view, the ability to implement robust control in the UAV hardware is addressed.

In spite of the efficient performance of the H_∞ – based robust control system, even after model order reduction, there are the high-frequency poles in the compensator transfer functions. It is difficult to implement these compensators in the current autopilot hardware. In other words, for digital implementation of designed filters, simplification and discretization lead to instability filters based on the maximum possible discretization frequency for autopilot hardware. This makes it impossible to implement these transfer functions. Therefore, two possible solutions are used to solve this problem: 1. The feasibility of developing an autopilot hardware for the ability to implement robust control based on mu-synthesis. 2. Design of a robust control system that can be implemented in existing hardware.

Table 1

Stages of the robust control development

Year	Developer	Field
1932	Nyqueist	Finding stability property of the system with negative feedback
1940	Bode	Developing stability property of the system with negative feedback with phase and gain concepts
1959	Horowitz	Introduction of quantitative feedback theory for uncertain system for SISO
1960 ten yeas	Kalman and Wiener	Introduction and development of state space for stochastic process and H2 optimization (LQG)
1981	Zames	Introduction of H_∞ and frequency domain concepts for presenting of uncertainties for MIMO
1984	Doyle	Development of frequency concepts introduced by Zames and state space methods for optimization
1989	Doyle, Glover, Khargonkar, Francis	H_∞ solution with algebraic Riccati equation
1992	MacFarlane and Glover	Loop shaping method
1992	Doyle	Structured singular value for robust performance problem solution
1994	Apkarian, Gahinet, Iawasaki, Skelton	Introduction of flexible Linear Matrix Inequality (LMI) method instead of Riccati equations

In the second part, the problem is stated. In the third section, the design of the control system based on mu- synthesis are discussed. In the third section, a feasibility study on the implementation of the control system based on the mu-synthesis is carried out. In the following sections, robust proportional integral derivative (PID) control is discussed. In Section VI, the results of the flight test for robust adaptive PID control for the roll channel of the Skywalker X8 flying wing (SX8FW) are presented. Eventually, in the seventh section, conclusions and suggestions for future works are presented.

Body-axis and Wind-axis Reference Frames for SX8FW and its airframe parameters are shown in fig. 1 and Table 2 respectively, [9–10].

The motion of the SX8FW is controlled by elevons, moved by an automatic control system. Differentially angular deflection of the right (δ_{er}) and left (δ_{el}) elevons has the same effect as aileron (δ_A) and commonly angular deflection of them has the same effect as elevator (δ_E), [10–11]:

$$\begin{bmatrix}\delta_E\\ \delta_A\end{bmatrix}=\begin{bmatrix}1 & 1\\ 1 & -1\end{bmatrix}\begin{bmatrix}\delta_{er}\\ \delta_{el}\end{bmatrix}. \quad (1)$$

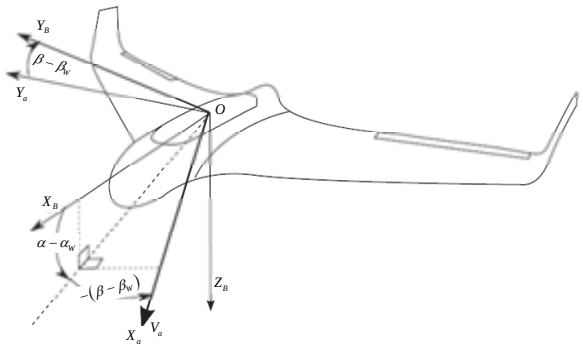

Fig. 1. Body-axis and Wind-axis reference Frames of the UAV

Table 2

Airframe parameters for SX8FW

Parameter	**Sky walker X8**
Mass: $m\left[kg\right]$	4.5
Moment of inertia: $J_x\left[kg.m^2\right]$	0.45
Moment of inertia: $J_y\left[kg.m^2\right]$	0.325
Moment of inertia: $J_z\left[kg.m^2\right]$	0.75
Moment of inertia: $J_{xz}\left[kg.m^2\right]$	0.06
Wing area: $S\left[m^2\right]$	0.75
Wing span: $b\left[m\right]$	2.12
Mean aerodynamic chord: $c\left[m\right]$	0.3571
Propeller area: $S_{prop}\left[m^2\right]$	0.1018
Air density: $\rho\left[kg/m^3\right]$	1.2682
Motor constant: K_{Motor}	40
Propeller aerodynamic coef.: C_{prop}	0.5

Nonlinear dynamical equations of the motion in the presence of the wind can be write as, [10]:

$$\begin{aligned}
&\left[\dot{V}_A\right]_B = \\
&\frac{f_{B-aero}+f_{B-thrust}(\delta_T)}{m(t)}+ \\
&H_I^B g_I-\omega_B\times\left[V_I\right]_B; \\
&f_{B-aero}=f_{B-aero}\left(|V_A|,\alpha-\alpha_W,\beta-\beta_W,\omega_B,\delta_A,\delta_E,\delta_R\right); \\
&\frac{d\omega_B}{dt}=I_B^{-1}\times \\
&\left(m_{B-aero}+m_{B-thrust}(\delta_T)-\omega_B\times I_B\omega_B\right); \\
&m_{B-aero}=m_{B-aero}\left(|V_A|,\alpha-\alpha_W,\beta-\beta_W,\omega_B,\delta_A,\delta_E,\delta_R\right); \\
&\frac{d\Theta}{dt}=L_B^E\omega_B,
\end{aligned} \tag{2}$$

where f_{B-aero}, $f_{B-thrust}$, m_{B-aero} and $m_{B-thrust}$ are aerodynamic and thrust forces and moments in the UAV Body Frame, α_W, β_W are angles of attack and side slip, α_W, β_W are angles of attack and side slip angle due to wind, V_A, V_I are airspeed and ground speed, ω_B is angular velocity vector; $\delta_A, \delta_E, \delta_R, \delta_T$ are control signals for aileron, elevator, rudder and thrust, g_I is the gravity vector in the Inertial Frame; I_B is matrix of inertial moments, Θ is vector of the Euler angles, H_I^B and L_B^E are the corresponding rotation matrixes. It means that aerodynamic forces and moments depend on airspeed where:

$$V_A = V_I - W = \begin{bmatrix} v_1 \\ v_2 \\ v_3 \end{bmatrix}_I - \begin{bmatrix} W_1 \\ W_2 \\ W_3 \end{bmatrix}_I;$$

$$\left[V_A\right]_B = \begin{bmatrix} u_A \\ v_A \\ w_A \end{bmatrix} = H_I^B V_A = V_B - H_I^B W; \tag{3}$$

$$\begin{bmatrix} |V_A| \\ \beta_A \\ \alpha_A \end{bmatrix} = \begin{bmatrix} \sqrt{{u_A}^2+{v_A}^2+{w_A}^2} \\ \sin^{-1}\left(v_A/V_A\right) \\ \tan^{-1}\left(w_A/u_A\right) \end{bmatrix},$$

where W is the wind vector in the Inertial Frame. The linearized lateral equations of motion, including the effect of the wind gusts, are:

$$\begin{aligned}
&\Delta x_{LatB} = \left[\Delta v \quad \Delta p \quad \Delta r \quad \Delta\phi\right]^T; \\
&\Delta u_{Lat} = \Delta\delta_A;\ \Delta w_{Lat} = \Delta v_W; \\
&\Delta\dot{x}_{LatB} = A_{lat}\Delta x_{LatB} + B_{lat}\Delta u_{Lat} + E_{lat}\Delta w_{Lat}; \\
&\Delta y_{LatB} = C_{lat}\Delta x_{LatB} + D_{lat}\Delta u_{Lat} + F_{lat}\Delta w_{Lat};
\end{aligned} \tag{4}$$

where matrixes A_{lat}, B_{lat}, E_{lat}:

$$A_{lat} = \begin{bmatrix} Y_v & Y_p + w_0 & Y_r - u_0 & g_I\cos\theta_0 \\ L_v & L_p & L_r & L_\phi \\ N_v + Y_v N_{\dot{v}} & N_p + \left(Y_p + w_0\right)N_{\dot{v}} & N_r + \left(Y_r - u_0\right)N_{\dot{v}} & 0 \\ 0 & 1 & -\sin\theta_0 & 0 \end{bmatrix};$$

$$B_{lat} = \begin{bmatrix} Y_{\delta A} \\ L_{\delta A} \\ N_{\delta A} + Y_{\delta A} N_{\dot{v}} \\ 0 \end{bmatrix},\ E_{lat} = \begin{bmatrix} -A_{lat}(1,1) \\ -A_{lat}(2,1) \\ -A_{lat}(3,1) \\ 0 \end{bmatrix} = \begin{bmatrix} -Y_v \\ -L_v \\ -\left(N_v + Y_v N_{\dot{v}}\right) \\ 0 \end{bmatrix}. \tag{5}$$

Where all of the parameters Y_v, Y_p, Y_r, L_v, L_p, L_r, L_ϕ, N_v, N_p, N_r and $N_{\dot{v}}$ depend on aerodynamic ones and matrixes C_{lat}, D_{lat}, F_{lat}:

$$C_{lat} = \begin{bmatrix} 1 & 0 & 0 & 0 \\ 0 & 1 & 0 & 0 \\ 0 & 0 & 1 & 0 \\ 0 & 0 & 0 & 1 \end{bmatrix};$$

$$D_{lat} = F_{lat} = \begin{bmatrix} 0 & 0 & 0 & 0 \end{bmatrix}^T. \tag{6}$$

For the SX8FW, aerodynamic parameters and their uncertainty are estimated based on actual flight data, Table 3, [9; 12–13]. The range of changes in the airspeed of the SX8FW is $18\text{m/sec} \pm 25\%$. It is worth noting that the uncertainty of the aerodynamic parameters is a little changed to better illustrate the difference between the robust control systems.

Table 3

Aerodynamic parameters estimates and their deviations for SX8FW

Parameters	Values	
	Estimated values (Uncertainty)	Theoretically values
C_{Y_β}	-0.0811 (60%)	-0.1949
$C_{Y_{\delta_a}}$	-0.0729 (80%)	-0.0696
C_{l_β}	-0.1170 (50%)	-0.0765
C_{l_p}	-0.3507 (30%)	-0.4018
C_{l_r}	0.0830 (90%)	0.0250

The end of tabl. 3

$C_{l_{\delta_a}}$	0.3087 (40%)	0.2987
C_{n_β}	0.0583 (60%)	0.0403
C_{n_p}	-0.0154 (50%)	-0.0247
C_{n_r}	-0.1023 (30%)	-0.1252
$C_{n_{\delta_a}}$	-0.002 (80%)	-0.0076

The goal is to design a robust control system for the lateral channel of the SX8FW in the presence of parametric uncertainties as well as changing the airspeed. The performance criteria of the control system are:

1. Maximum rejection of parametric and dynamic uncertainties and external disturbances effect on the roll and course angles ϕ, χ. If the wind is not present, the course angle is equal to the yaw angle.

2. Tracking of the course reference angle in the presence of parametric and dynamic uncertainties and external disturbances with the favorable phase and gain margins.

3. Fulfillment of the above conditions in the presence of the angle and rate constraints on the aileron deflection.

Robust control based on mu-synthesis

The closed-loop system structure, which is commonly used for robust control design, is shown in Fig. 2. The most time-consuming part of the robust control system design based on mu-synthesis is to adjust the weight functions associated with reference tracking, disturbance rejection, and control effort to reconcile the various requirements of the system.

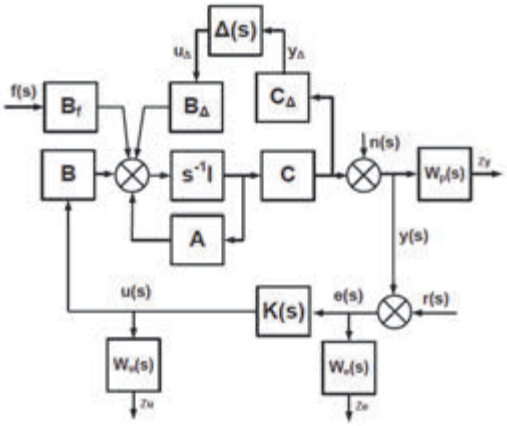

Fig. 2. General robust control block diagram

Method of mu-synthesis for robust control design results in high-order transfer functions. For the purposes of implementation, the order of the model should be reduced. The high-order, stable, and time-invariant model for irreducible realization controller is given. In the process of decreasing the control order $C(s)$, the aim is to remove the high frequency and very fast modes and find a low-level controller $C_r(s)$ so that the H_∞ Norm $\|C(s)-C_r(s)\|_\infty$ is extremely small. The order of the model is equal to the number of states in the irreducible realization, sometimes known as the MacMillan order. In order to reduce the order of the model, the following methods can be used:

1. Balanced Truncation.
2. Balanced Residualization.
3. Optimal Hankel Norm estimation.

In the balanced truncation method, the high-frequency characteristics of the transfer function are preserved in the order reduction process, and in contrast, in the Balanced Residualization method, the features of the transfer function at low frequencies are maintained. These two order reduction methods are converted to each other by bilinear transformation. Henkel singular values represent the energy of states in the system. If low energy modes are eliminated when reducing the order of magnitude, then the features of the system will be further preserved. The Henkel singular values can be interpreted as follows:

$$\sigma_H = \sqrt{\lambda_i(PQ)} \qquad (7)$$

Where P and Q and are controllability and observability Gramians. Henkel singular values can be calculated with the command hackelsv in MATLAB program.

However, due to the limitations of the existing autopilot, this reduced order controller model also can not be implemented.

Roll and course angles and aileron control signal of the SX8FW for the Monte Carlo simulation of the lateral motion with robust control based on mu-synthesis are shown in Fig. 3. The properties of course angle reference signal tracking and eliminating the disturbance effect on the roll and course angles for the uncertain system in the presence of the control signal constraint are satisfied.

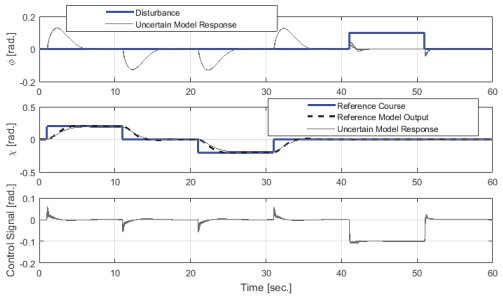

Fig. 3. Roll and course angles and aileron control signal of the SX8FW for the Monte Carlo simulation of the lateral motion with robust control based on mu-synthesis

Feasibility study on the implementation of the robust control based on the mu-synthesis

In spite of the effective efficiency of the robust control based on mu-synthesis and model order reduction, there are still some high-frequency modes in this controller that make it impossible to implement them in autopilot hardware, [14]. In other words, for digital implementation of designed filters, simplification and discretization lead to instability filters based on the maximum possible discretization frequency (300 Hz) for autopilot hardware.

The robust control transfer functions designed for the roll channel are as follows:

$$\sigma_H = \sqrt{\lambda_i (PQ)}\,. \qquad (8)$$

Therefore, two possible solutions have been used to solve this problem: 1. Feasibility study of autopilot hardware development to enable the implementation of robust control based on synthesis. 2. Design of a robust control system that can be implemented in existing hardware.

The following methods can be used to develop the autopilot hardware to enable the implementation of robust control based on mu-synthesis:

1. Manipulate designed robust control filters and reduce the order of the poles to allow the implementation of filters.

2. Split each filter to achieve stable digital filters for implementation.

3. Using a dual-core microcontroller or two microcontrollers to increase its speed and functionality to enable the implementation of designed filters.

A more practical and faster solution to implement a robust control system in the existing autopilot hardware is the design of a different robust control system. The existing unmanned aerial vehicle control system is composed of PID controllers. Therefore, based on an uncertain dynamics model identified from the flight test information, two PID controllers are designed: 1. Robust PID control (robust to the uncertainty of aerodynamic parameters, UAV airspeed changes, and external disturbances). 2. A adaptive robust PID controller (robust to the uncertainty of aerodynamic parameters of the UAV and external disturbances and adaptive based on the UAV airspeed) are designed.

Robust PID for the UAV

In order to design the robust PID in the presence of the control signal and its rate limitations the following conditions are satisfied:

1. Reference tracking in the presence of the system uncertainties and external disturbances.

2. Disturbance rejection for the roll and course angles in the presence of the uncertainties and external disturbances.

Robust PID controller meets closed loop stability, adequate performance and robustness and achieves a good balance between performance and robustness.

The block diagram of the UAV lateral dynamic with the internal and external loops and robust PID controllers is depicted in Fig. 4. The control system generates a control signal that satisfies the actuator angle and rate limitations. Six parameters of the robust PID controllers are achieved in the design process based on optimization. In Fig. 5 to Fig. 7, the ability command signal following and disturbance rejection in the Monte Carlo simulation of the UAV was shown for the usual PID control and robust PID controller. It can be seen that the PID, based on the nominal model leads to unstability in the presence of some uncertainties that makes roll angle fluctuation and control signal saturation.

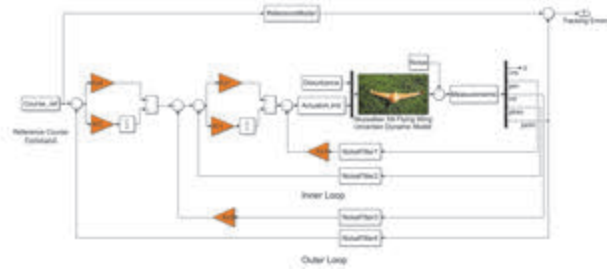

Fig. 4. Closed loop system of the UAV uncertain lateral dynamics with robust PID contollers

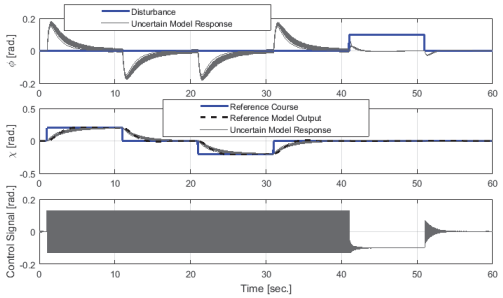

Fig. 5. Instability and saturation of the control signal in tracking the reference signal and eliminating disturbances in the Monte Carlo simulation of the SX8FW for the typical PID

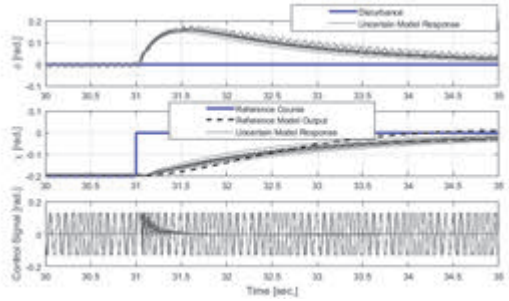

Fig. 6. Instability and saturation of the control signal in tracking the reference signal and eliminating disturbances in the Monte Carlo simulation of the SX8FW for the typical PID (zoomed)

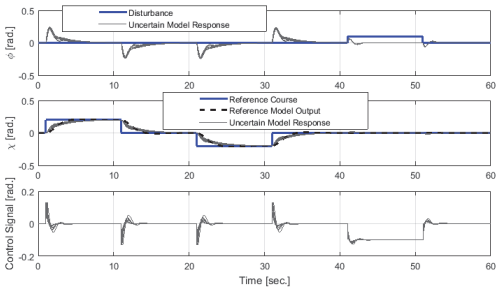

Fig. 7. Ability of reference signal tracking and disturbance rejection in the Monte Carlo simulation of the SX8FW for the robust PID control system

Flight test with adaptive robust PID for the roll channel

The UAV dynamic model is also a function of the airspeed. Airspeed is measured during flight. It is possible to use airspeed and design an adaptive PID regulator. From the practical point of view, in the event of a large change in the airspeed such as in the passenger aircraft, in order to effectively control it, the flight vehicle control actuators or its aerodynamic configuration also must be adapted to match the airspeed. It is worth noting that due to the dependency of the flight vehicle dynamics to the airspeed, control system of the airspeed is also designed, [2].

In this section, flight test results are presented for controlling the roll channel with adaptive robust PID. Adaptive robust PID controller for the roll channel has the following structure:

$$C_{adaptive}(s) = \begin{bmatrix} K_P(V_a) + K_I(V_a)/s \\ K_D(V_a) \end{bmatrix} \Rightarrow$$
$$U(s) = \begin{bmatrix} K_P(V_a) + K_I(V_a)/s \\ K_D(V_a) \end{bmatrix} \begin{bmatrix} \varphi_{ref}(s) - \varphi(s) \\ P(s) \end{bmatrix}. \quad (9)$$

Where the coefficients of the adaptive robust PID controller are the functions of the airspeed of the UAV. In Fig. 8, flight test results are shown with the adaptive robust PID for the roll channel. As can be seen, the effect of disturbances on the roll channel is reduced by the adaptive robust PID controller (from 120 s to 290 s).

The controller is evaluated for speeds of 11 and 15 m/s. For parts of flight information where the SX8FW has a roll angle of zero and SX8FW flies straight, the angular velocity of the roll is calculated. The roll angular velocity variance, as disturbance effect indicator, is decreased by about 20% with adaptive robust PID control relative to PID control.

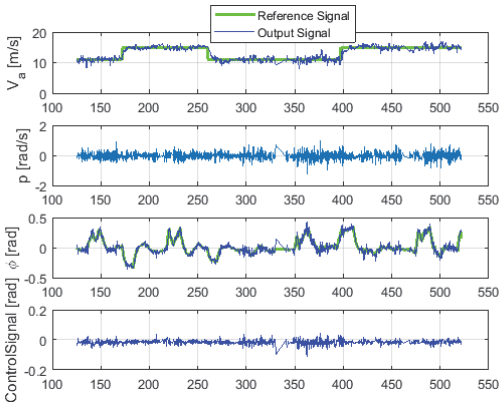

Fig. 8. Flight test results for the roll channel, with adaptive robust controller (from 120 s to 290 s), with conventional PID controller (from 290 s later)

Conclusion

In this paper, a robust control system based on three methods of mu-synthesis, a robust PID control and an adaptive robust control using optimization for an uncertain model of an unmanned air vehicle was designed. The robust controller based on the mu-synthesis had better performance than PID controllers. To implement the robust control based on mu-synthesis, it was proposed to modify the autopilot hardware structure and use two parallel microcontrollers or a dual-core microcontroller. An adaptive robust PID based on the considerations of the quality and the robustness, as well as hardware considerations, was designed and implemented in the existing autopilot for the roll channel. It showed better performance than conventional PID controller in the flight test. Implementation of the robust control based on mu-synthesis as well as the adaptive robust PID controller for lateral dynamics can be done in the future works.

References

1. Holtsov, A., Farhadi, R., Kortunov, V. and Mohammadi, A. (2016), Comparison of the UAV adaptive control with the robust control based on mu-synthesis, *Methods and Systems of Navigation and Motion Control (MSNMC), 2016 4th International Conference on*, pp. 18-21: IEEE.

2. Farhadi, R.M., Kortunov, B.I. and Mohammadi, A. (2015), Robust control design for the airspeed of UAV, *Actual Problems of Unmanned Aerial Vehicles Developments (APUAVD), 2015 IEEE International Conference*, pp. 145-148: IEEE.

3. Lavretsky, E. and Wise, K.A. (2013), *Robust and Adaptive Control*, Springer, pp. 317-353.

4. Balas, G., Chiang, R., Packard, A. and Safonov, M. (2007), *Robust Control Toolbox 3: User's Guide*, Mathworks, Natick, MA.

5. Gu, D.-W., Petkov, P. and Konstantinov, M.M. (2005), *Robust control design with MATLAB®*. Springer Science & Business Media.

6. Colgren, R.D. (2004), *Applications of robust control to nonlinear systems*, AIAA.

7. Melnik, A.T.K., Melnik, K. and Tunick, A. (2009), Designing multidimensional robust flight control systems based on H∞-optimization and μ-synthesis procedures, *Informational systems, mechanics and control: science-technical Journal*, vol. 3, pp. 40-57.

8. Farhadi, R.M., Kortunov, V.I. and Mohammadi, A. (2016), Robust control of the UAV with mini autopilot, *2016 23rd*

Saint Petersburg International Conference on Integrated Navigation Systems (ICINS), Sang Peterburg, 2016.

9. Gryte, K. (2015), *High Angle of Attack Landing of an Unmanned Aerial Vehicle*, NTNU.
10. Stengel R.F. (2015), *Flight dynamics*, Princeton University Press.
11. Beard, R.W. and McLain, T.W. (2012), *Small unmanned aircraft: Theory and practice*, Princeton university press.
12. Farhadi, R.M. and Kortunov, V.I. (2017), " Identifikaciya dinamiki kanala krena bespilotnogo letatel'nogo apparata pri slabo informativnom vxodnom signale" [Identification of roll channel dynamics for the unmanned aerial vehicle under weakly excited input signal], *Radioelectronic and Computer Systems*, vol. 1, no. 1, pp. 99-106.
13. Farhadi, R.M., Kortunov, V.I., and Mohammadi, A. (2015), UAV motion model and estimation of its uncertainties with flight-test data, *22rd Saint Petersburg International Conference on Integrated Navigation Systems*, pp. 131-133.
14. Kortunov, V., Mazurenko, O.V., Gorbenko, A.V., Mohammed, W., and Hussein, A. (2015), Review and comparative analysis of mini- and micro-UAV autopilots, *Actual Problems of Unmanned Aerial Vehicles Developments (APUAVD), 2015 IEEE International Conference*, Kiev, Ukraine, pp. 284-289: IEEE.

Надійшла до редколегії 19.07.2017
Схвалена до друку 21.09.2017

Відомості про авторів:
Мохаммаді Фархаді Рахман
Аспірант
Національний аерокосмічний університет
ім. Н.Є. Жуковського "ХАІ", Харків, Україна
orcid.org/ 0000-0002-9038-8154
e-mail: rmfarhadi.ua@gmail.com

Кортунов В'ячеслав Іванович
Доктор технічних наук професор,
Національний аерокосмічний університет
ім. М.Є. Жуковського "ХАІ", Харків, Україна
orcid.org/0000-0003-3960-6037
e-mail: v.kortunov@khai.edu

Information about the authors:
Mohammadi Farhadi Rahman
Postgraduate Student of
National Aerospace University,
Kharkiv, Ukraine
orcid.org/0000-0002-9038-8154
e-mail: rmfarhadi.ua@gmail.com

Kortunov Vyacheslav
Doctor of Technical Sciences Professor,
National Aerospace University,
Kharkiv, Ukraine
orcid.org/0000-0003-3960-6037
e-mail: v.kortunov@khai.edu

ПРОЕКТУВАННЯ І ТЕСТУВАННЯ РОБАСТНОГО УПРАВЛІННЯ В МІНІ АВТОПІЛОТІ БПЛА

Р. М. Фархаді, В.І. Кортунов

В статті представлені три розроблені методи синтезу робастних систем управління для невизначеної динамічної моделі безпілотного літального апарату, а саме: на основі методу мю-синтезу, методу робастного пропорційно-інтегрально-похідного управління та методу робастно-пропорційно-інтегрально-похідного управління з використанням оптимізації. Були досліджені можливості реалізації розроблених робастних систем управління автопілотом для самольоту типу моно-крило. Показано, що робота системи управління на основі мю-синтезу може досягати кращого спостереження опорного сигналу та придушення збурень. Для реалізації системи управління, заснованої на мю-синтезі, у вигляді складності регулятора необхідно використовувати два паралельні мікроконтролери або двоядерний мікроконтролер. Розроблені адаптивний робастний і робастний пропорціонально-інтегрально-похідний компенсатор для каналу крена, використаний в автопілоті и протестований в реальних польотах. Результати льотних випробувань з адаптивним робастним компенсатором показують більше придушення збурень у каналі крену, ніж зі традиційним.

Ключові слова: *робастне управління, мю-синтез, безпілотний літальний апарат, адаптивний робастний пропорційно-інтегрально-похідний компенсатор, автопілот, робастна система управління.*

ПРОЕКТИРОВАНИЕ И ТЕСТИРОВАНИЕ РОБАСТНОГО УПРАВЛЕНИЯ В МИНИ АВТОПИЛОТЕ БПЛА

Р.М. Фархади, В.И. Кортунов

В статье представлены разработанные три метода синтеза робастных систем управления для неопределенной динамической модели беспилотного летательного аппарата, а именно: на основе метода мю-синтеза, метод робастного пропорционально-интегрально-производного управления и метод робастно-пропорционально-интегрально-производного управления с использованием оптимизации. Была исследована возможность реализации разработанных робастных систем управления в автопилоте для самолета типа моно-крыло. Показано, что робастная система управления на основе мю-синтеза может достичь лучшего слежения опорного сигнала и подавления возмущений. Для реализации системы управления, основанной на мю-синтезе, в виду сложности регулятора необходимо использовать два параллельных микроконтроллера или двухъядерный микроконтроллер. Разработаны адаптивный робастный и робастный пропорционально-интегрально-производный компенсатор для канала крена, который реализован в автопилоте и испытан в реальных полетах. Результаты летных испытаний с адаптивным робастным компенсатором показывают большее подавление возмущений в канале крена, чем с традиционным.

Ключевые слова: *робастное управления, мю-синтез, беспилотный летательный аппарат, адаптивный робастный пропорционально-интегрально-производный компенсатор, автопилот, робастная система управления.*